International Journal of Offshore and Polar Engineering (ISSN 1053-5381)

Vol. 16, No. 3, September 2006, pp. 1–7

Prediction of Deepwater Oil Offloading Buoy Response and Experimental Validation

Sangsoo Ryu*, Arun S. Duggal*, Caspar N. Heyl and Yonghui Liu
FMC Technologies Floating Systems Inc., Houston, Texas, USA

Fully coupled time-domain approaches were applied to predict the vertical plane motions, i.e. surge, heave and pitch, of the deepwater buoy. It is found that the pitch motion in particular is sensitive to the drag effect of the skirt, and is coupled with both surge and heave motions, and that a time-domain fully coupled analysis can capture the viscous drag effect. Results from 2 experiments, one with a freely floating buoy and the other with a moored buoy, are presented to show that the proposed time-domain coupled analysis predicts the buoy motion behavior very well for both cases compared to frequency-domain analyses with a linearized stiffness for the mooring system. Comparison of experimental data and coupled analysis results from the proposed buoy skirt modeling with multiple disks shows that viscous modeling of the buoy skirt by applying a Morison drag force formulation based on relative velocity can be used to better predict the pitch motion.

INTRODUCTION

Since the first catenary anchor leg mooring (CALM) system was employed in 1961, this system has been extensively applied as a loading/offloading terminal (Hwang, 1997). As the current major oil and gas fields are getting depleted, new potential fields in deep and ultra-deep seas are getting more and more attention (Ryu and Kim, 2003). This results in developing the CALM buoy system in deep waters, an application whose dimensions and hydrodynamic characteristics differs from that in shallow waters.

Deepwater offloading buoys are being extensively used in West Africa to allow efficient loading of spread-moored FPSO. Some of the current projects of the offloading buoys include Agbami (Nigeria, 1435-m water depth), Akpo (Nigeria, 1285-m), Bonga (Nigeria, 1000-m), Dalia (Angola, 1341-m), Erha (Nigeria, 1190-m), Girassol (Angola, 1320-m), Greater Plutonio (Angola, 1310-m) and Kizomba A & B (Angola, 1200-m and 1000-m).

Deepwater offloading buoys have a relatively small displacement when compared to other floating systems such as TLP, spar and FPSO, with the majority of the displacement being used to support the mooring system and the oil offloading lines. This results in a floating system that has a very active response to the environment, coupled with feedback from the mooring and flowline systems. In addition, compared to other floating systems, deepwater offloading buoy systems have relatively unique system identifiers (i.e. inertia, damping and stiffness). In other words, the orders of the total mass of the mooring lines and oil offloading lines (OOL), the viscous damping due to a skirt, and the stiffness from the mooring lines and hawsers are considerable compared to those of the inertia, radiation damping and hydrostatic stiffness of the buoy, respectively.

As the operating water depth increases, prediction of full 6 degree-of-freedom (DOF) motions of the offloading buoy becomes more difficult because the mass/damping/stiffness contribution of mooring system and oil offloading lines becomes even more influential than that of the buoy. Thus, the coupling between mooring lines/oil offloading lines and the buoy hull becomes more complex.

A time-domain coupled analysis of a CALM system was performed based on both radiation/diffraction and Morison's equation (Sagrilo et al., 2002). In that work only statistical results—such as mean value, standard deviation and most probable 3-h maximum value, for surge, heave and pitch of a CALM buoy and 6 mooring lines—were calculated and compared to available model test results. However, the RAO of those 3 buoy motions in a vertical plane were not directly compared to the model test results. As the riser/mooring/hull coupling becomes more significant in deeper waters, the coupled analysis is emphasized to better predict the motion of the floater and line dynamics (Ormberg and Larsen, 1998). Frequency-domain coupled analysis was discussed in terms of computational efficiency without loss of accuracy compared to time-domain coupled analysis of floating production systems (Garret, 2005).

Cable-buoy coupled motions of 3 different types of tethered buoys (disc, sphere and spar buoy) were studied (Leonard et al., 2000). Because the buoy pitch motion is less accurate than the other 2 motions, i.e. heave and surge (Leonard et al., 2000; Sagrilo et al., 2002), more accurate pitch motion prediction is required to better assess other buoy design issues such as fatigue life.

The motion behavior of this buoy system has been shown to result in severe fatigue damage to the mooring and flowline components (Heyl et al., 2001), and thus must be estimated accurately to ensure that the system is designed with sufficient fatigue life.

In a deepwater buoy system it is necessary to identify and implement the effect of both inertia and viscous loadings on each object of the buoy system, as the fundamental natural periods of the buoy are in the range of 1st-order wave loading, and the system is sensitive to damping. Bunnik et al. (2002) conclude that the pitch motion cannot be well predicted when the viscous effects of the skirt are neglected. Cozijn and Bunnik (2004) also found that the pitch motions were overpredicted and suggested that this may come from nonlinear viscous effects in the wave exciting pitch moment.

In this study, in order to accurately predict the buoy pitch motion by applying the Morison equation as the viscous effect, a fully coupled time-domain analysis and a diffraction model of the buoy with viscous drag elements are employed. This paper's

*ISOPE Member.

Received August 10, 2005; revised manuscript received by the editors July 21, 2006. The original version (prior to the final revised manuscript) was presented at the 15th International Offshore and Polar Engineering Conference (ISOPE-2005), Seoul, June 19–24, 2005.
KEY WORDS: Deepwater oil offloading buoy, coupled analysis, floating body dynamics, mooring analysis, Morison equation.

main objective is to show the development of a numerical model to better predict the pitch motion, in particular, of the buoy by implementing a new way of skirt modeling based on drag elements.

Results from time- and frequency-domain calculations of the deepwater offloading buoy system are presented. The results are also compared to results of model tests of a freely floating buoy and a moored buoy to validate the computational methods and the suggested buoy modeling being employed to predict the buoy motions. The results and comparisons demonstrate the importance of accounting for the viscous modeling of a buoy skirt. Results from sensitivity studies are also presented to show the importance of the contribution of a skirt in predicting motion response amplitude operators (RAO).

DESCRIPTION OF MODEL TEST

The model test program was specifically designed to study the deepwater buoy on a large scale. Due to the large typical prototype depth (greater than 1000 m) and the limitation of the basin facility, the decision was made to model the buoy and the environment on a large model scale. The mooring system was represented by a simplified anchor leg system that resulted in similar stiffness and natural periods as a prototype buoy in 1000 m of water (Colbourne, 2000).

Two sets of model tests were performed: a freely floating buoy (very soft springs used) and a moored one. The freely floating tests were designed to provide data for the response of the buoy with no mooring influence so as to allow direct validation of the buoy hull model response. The second set of tests was performed with a simplified mooring system to provide data for the response of the buoy influenced by the mooring system. Model tests were conducted in the Offshore Engineering Basin at the Institute for Marine Dynamics in Canada.

Model Basin

The tank is 75 m long by 32 m wide with a variable water depth of up to 3 m (Fig. 1). The wavemakers consist of 168 rectangular panels across the front of the tank and along the side in an L-shaped formation.

Model

The buoy hull for the test is modeled at a scale of 1:35.6. For the first set of tests in a horizontal mooring system, the buoy was ballasted to have a free-floating draft of 5.65 m. For the second set of tests, the pretension of the mooring system resulted in a draft of 5.65 m. The model is fitted with a skirt with 18 holes. Mooring lines were terminated at load cells to measure the mooring tension at the skirt. All instrument cables were routed out of the buoy

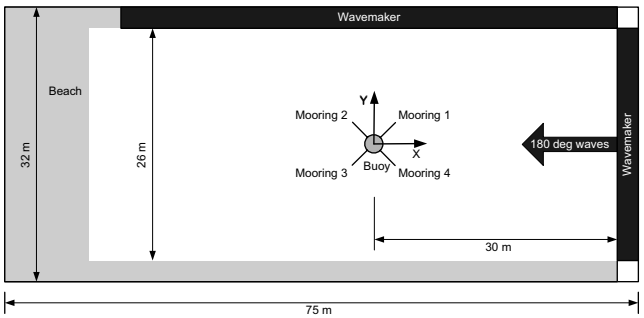

Fig. 1 Plan view of experimental configuration of deepwater buoy

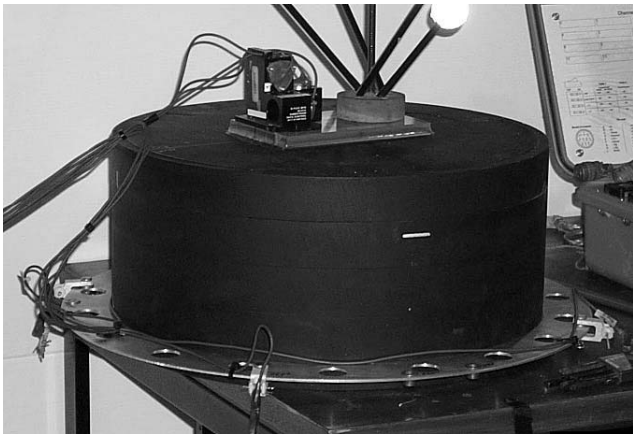

Fig. 2 Deepwater buoy model

model through a suspended umbilical cable (Fig. 2). Table 1 lists the buoy particulars for both cases.

Mooring Configurations

The first mooring configuration was designed to investigate the motions of a freely floating buoy with minimal influence of the mooring system. The horizontal mooring system consisted of 4 lines with soft springs that maintained the buoy at the desired location but had minimal feedback to the wave frequency motions. The second mooring system configuration was designed to have the stiffness characteristics and pretension of a 1000-m mooring system for an offloading buoy. To simplify the mooring (and its modeling), the mooring was represented by 4 legs spaced 90° apart, with fairlead angles of 45°. The pretension was designed to provide the net mooring and offloading system load on the buoy (to give the desired draft of 5.65 m). The mooring system was further simplified to be as light as possible with minimal drag so that the stiffness was the primary influence on the buoy response. Table 2 gives the details of the 2 systems.

MATHEMATICAL FORMULATION AND MODELING

The modeling of a deepwater buoy is complex due to the coupling between buoy, mooring and flowlines. In addition, the viscous forces, due to the interaction of the environment (fluid) with the hull, mooring and flowlines, further complicate the analysis of the system. However, the objective of the current study is to

	Unit	Mooring 1	Mooring 2
Model Test Scale		35.6	35.6
Water Depth	m	106.8	106.8*
Buoy Hull Diameter	m	17.0	17.0
Skirt Diameter	m	21.0	21.0
Buoy Height	m	7.65	7.65
Draft	m	5.65	5.65
Weight in Air	ton	1293.2	878.6
KG	m	3.84	3.40
Buoy Total Rxx	m	3.82	4.39
Buoy Total Ryy	m	3.82	4.39
Fairlead Radius	m	9.50	9.50
No. of Mooring Legs		4	4

Note that equivalent water depth for mooring 2 is 1000 m.

Table 1 Buoy model particulars

	Unit	Mooring 1	Mooring 2
Length	m	350	133.3
Wet Weight	kg/m	NA	3
Diam	mm	NA	NS
EA	metric tons	180	1963
Pretension	metric tons	22	150
Fairlead Angle	deg	0	45

Table 2 Particulars of 2 mooring configurations

focus on the accurate modeling of the fluid interaction with the buoy hull, accounting for both the inertia and viscous forces on the buoy.

To accurately predict the motions of the buoy, a fully coupled time-domain analysis is applied, because the influence of the inertia and drag of the skirt for the motions of the buoy is one of the driving factors. We address an appropriate modeling of the buoy skirt drag and inertia effect and the estimation/implementation of the viscous damping of the buoy hull.

To consider coupling and interactions between a buoy and mooring lines, Eq. 1, the governing equation of the rigid-body dynamics of the buoy, is solved:

$$\{M + M_a(\infty)\}\ddot{\vec{X}} + \int_0^\infty R(t-\tau)\dot{\vec{X}}d\tau + K\vec{X} = \vec{F}_d + \vec{F}_w^{(1)} + \vec{F}_w^{(2)} + \vec{F}_{\text{line}} \quad (1)$$

where M and M_a represent the mass and added mass matrices; R, the retardation function matrix; K, the hydrostatic stiffness matrix; $\vec{X}$, the body displacement; $\vec{F}_d$, the drag force; $\vec{F}_w^{(1)}$ and $\vec{F}_w^{(2)}$, the 1st- and 2nd-order wave loads; $\vec{F}_{\text{line}}$, the interface loads from the mooring lines and the OOL; and the arrow above each variable, the column vector. To calculate $\vec{F}_{\text{line}}$, the virtual work principle was applied, and the governing equation of motion, including the buoy and the lines, is solved by Newmark's algorithm, which allows the expression of the unknowns, acceleration and velocity, as a function of displacement $\vec{X}$. More detailed description of the numerical formulation can be found in Principia (2004). The mooring system in this study was simplified as a spring element.

The drag damping in pitch/roll is known as a driving parameter in buoy responses. Consequently, for drag force calculations it is more physically reasonable to apply the relative velocity (buoy and water particles) than to use the absolute buoy velocity, as the buoy velocity has an order of values similar to that of surrounded water particles. Due to the moment arm effect, the pitch/roll response is significantly affected by the drag force caused by the skirt, especially in the range of pitch natural period. The heave response around the natural period is also controlled by the skirt drag/viscous effect.

Boundary Integral Equations

Assuming that the fluid has no viscosity, the boundary value problem can be solved as a velocity potential problem that satisfies the Laplace equation. Eq. 2 gives the total velocity potential:

$$\phi = \phi_D + \phi_R \quad (2)$$

where the diffraction potential ϕ_D is defined as the sum of the incident wave potential ϕ_I and the scattered potential ϕ_S. To calculate wave exciting loads, the added mass, and the potential damping based on the inviscid and irrotational fluid field, the radiation and diffraction potentials are obtained from boundary integral Eqs. 3 and 4. The total diffraction velocity potential ϕ_D can be expressed as Eq. 4 (Korsmeyer et al., 1988):

$$2\pi\phi_k(\vec{x}) + \iint_{S_B}\left(\phi_k(\xi)\frac{\partial G(\xi;\vec{x})}{\partial n_\xi} - n_k G(\xi;\vec{x})\right)d\xi = 0 \quad (3)$$

$$2\pi\phi_D(\vec{x}) + \iint_{S_B}\phi_D(\xi)\frac{\partial G(\xi;\vec{x})}{\partial n_\xi}\,d\xi = 4\pi\phi_I(\vec{x}) \quad (4)$$

where ϕ_k is the unit-amplitude radiation potential due to ξ_k, the complex amplitude of the oscillatory motion in mode k of the 6 DOF, S_B is the body boundary, and Green function $G(\xi;\vec{x})$ is the velocity potential at the point $\vec{x}$ due to a point source of strength -4π located at the point ξ.

A diffraction/radiation program is used to calculate the buoy 1st-order wave exciting loads, the added mass, and the radiation damping based on the equations noted above. These calculated values were used to solve Eq. 1 in time domain. The head wave condition and 36 wave periods from 0.5 s to 22 s were selected, and the corresponding 1st-order wave exciting loads in the vertical plane were calculated. To take into account the skirt effect on added mass and radiation damping, the skirt is included in the mesh generation for the radiation problem. The holes on the skirt were not meshed. These hydrodynamic results of the buoy alone are transferred to DeepLines, a fully coupled time-domain analysis program, to calculate the hull/mooring line coupled buoy motion and mooring analysis for both configurations.

Local Coordinate System Conventions

To conveniently describe 6-DOF buoy motions, an earth fixed coordinate system is used (Fig. 3). The line of wave propagation is chosen as the negative X, and Y-axis is 90° counter-clockwise from the X-axis. Z-axis is vertically upward, starting from the keel line of the buoy. Note that the center of gravity (CoG) of the buoy is located at (0 m, 0 m, 3.84 m) in this local coordinate

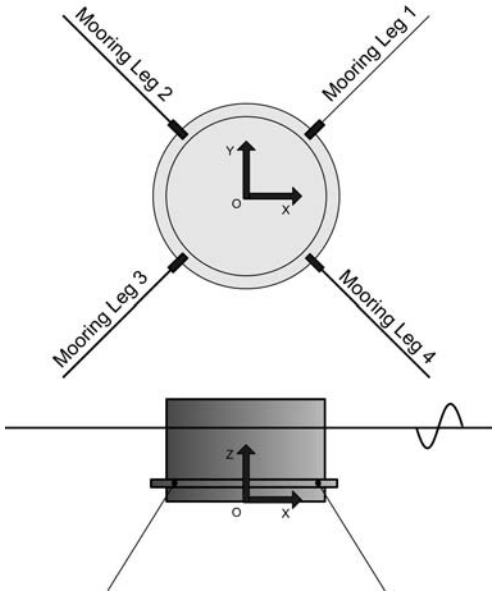

Fig. 3 Buoy local coordinate system

Mode	Surge	Sway	Heave	Roll	Pitch	Yaw
Surge	0	0	0	0	0	0
Sway	0	0	0	0	0	0
Heave	0	0	2.28e6	0	0	0
Roll	0	0	0	2.76e7	0	0
Pitch	0	0	0	0	2.76e7	0
Yaw	0	0	0	0	0	0

Table 3 Buoy hydrostatic stiffness matrix (in N/m, N and N-m)

system, and all the hydrodynamic coefficients are obtained with respect to the CoG. Followed are the detailed axis conventions:

- Wave elevation positive upward
- Surge (X-motion) along X-axis
- Sway (Y-motion) positive based on right-handed system
- Heave (Z-motion) positive upward
- Roll positive starboard down
- Pitch positive bow down
- Yaw positive bow to portside

Buoy Hydrostatic Stiffness

Table 3 summarizes the hydrostatic stiffness obtained at the CoG in the local coordinate system described above.

Consideration of Viscous Damping

The method for the viscous estimation of roll/pitch is based on Valliet et al. (2002), which states that the viscous damping of the buoy with a skirt is divided into 2 separate damping contributions. An analytic formula for a barge is applied for the damping from a buoy hull without a skirt:

$$C = \frac{1}{2}\rho C_d B^4 L\dot{\phi}|\dot{\phi}| \tag{5}$$

where ρ is water density; C_d, drag coefficient; B, beam; L, length; and $\dot{\phi}$, angular velocity. To apply this formula to a buoy, the definitions of parameters in Eq. 5 are shown in Fig. 4.

The associated total drag roll/pitch moment is derived as follows:

$$\begin{aligned} dM_{\text{hull}} &= \frac{1}{2}\rho C_d B^4 L\dot{\phi}|\dot{\phi}| \\ M_{\text{hull}} &= \int_0^{\pi} \frac{1}{2}\rho C_d (2R\sin\theta)^4 R\, d\theta\dot{\phi}|\dot{\phi}| \\ &= 3\pi\rho C_d R^5\dot{\phi}|\dot{\phi}|. \end{aligned} \tag{6}$$

To take into account viscous/drag effects caused by a skirt, Morison-type drag elements are implemented by using multiple disks (Fig. 5). Viscous coefficients $C_d = 0$, 30 and 50 were

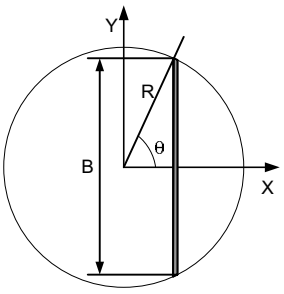

Fig. 4 Schematic diagram for mathematical derivation of roll/pitch damping

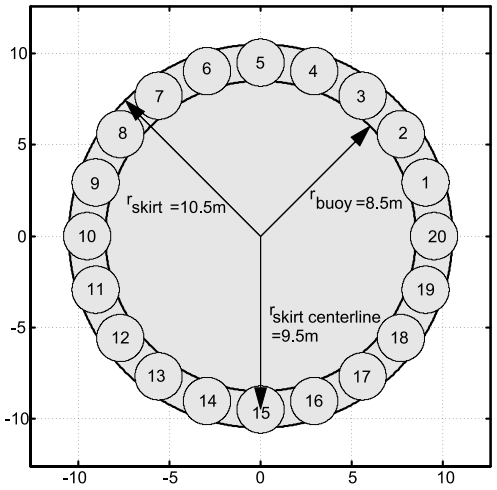

Fig. 5 Skirt modeling by use of multiple disks

applied, and heave and pitch motions were thoroughly investigated by comparing with model test results including free-decay tests.

Not only does the buoy skirt affect the added mass and radiation damping, but it generates either viscous damping and/or drag-induced exciting force depending on its relative velocity to the wave kinematics in the surrounded velocity field, because nonlinear drag force proportional to the relative velocity squared can contribute as both exciting and damping forces.

Because the skirt-induced added mass and inertia force are already taken into account in the radiation/diffraction problem, in a time-domain analysis only the viscous coefficient is included. The inertia coefficient of the disks was set to zero. Table 4 summarizes the detailed viscous/drag modeling in each 6-DOF direction.

MODEL TESTS VS. CALCULATIONS

A series of comparisons is made between the numerical simulations and the model test results. First, a comparison is made of the free-decay tests with both mooring configurations to provide a basic comparison of the numerical model and the model test data. This demonstrates the accuracy of the numerical model in capturing the damping in individual modes and the natural periods. The second set of comparisons focuses on the RAO of the buoy estimated from the model tests and the numerical simulations for both mooring configurations. The data are presented to allow comparison of both frequency- and time-domain models, and for both mooring configurations.

		Velocity Applied		Linear or Quadratic		
Mode		Absolute	Relative	Linear	Quadratic	Cd or D
Surge			√		√	1.2
Sway			√		√	1.2
Heave			√		√	6.0
Roll	Hull	√			√	8.56e8
	Skirt		√		√	50.0
Pitch	Hull	√			√	8.56e8
	Skirt		√		√	50.0
Yaw		√			√	1.20e6

Table 4 Summary of buoy viscous/drag modeling

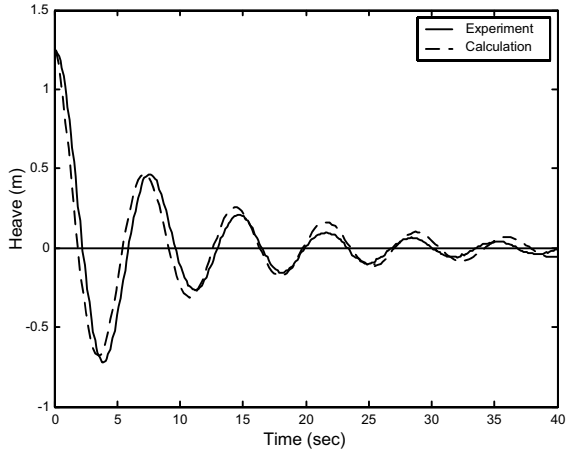

Fig. 6 Heave free-decay test for freely floating case: solid line = experiment, dashed line = calculation

Free-Decay Tests

Surge, heave and pitch free-decay experimental data and fully coupled time-domain calculations are compared and shown in Figures 6∼10 for both mooring configurations. As the surge free-decay motion of the freely floating buoy is an overdamped case, only heave and pitch free-decay tests are presented. Note that both the heave and pitch modes are strongly influenced by the skirt (added mass and damping), and that the numerical simulation accurately replicates the model test results. This demonstrates that the skirt model implemented in this paper is a good representation of the actual fluid-structure interaction.

Buoy Motion RAO

Comparisons are made for both mooring configurations: (1) a buoy in horizontal mooring whose stiffness is negligible (see Figs. 11∼13), and (2) a simplified mooring system with the stiffness characteristics of a mooring in 1000 m of water (see Figs. 14∼16). The motion RAO of the buoy were derived at the buoy CoG. Figs. 11∼16 present the buoy's vertical plane motion RAO, i.e. surge, heave and pitch. Both regular and irregular waves were used for the tests, and both frequency- and time-domain calculations were conducted as a comparison.

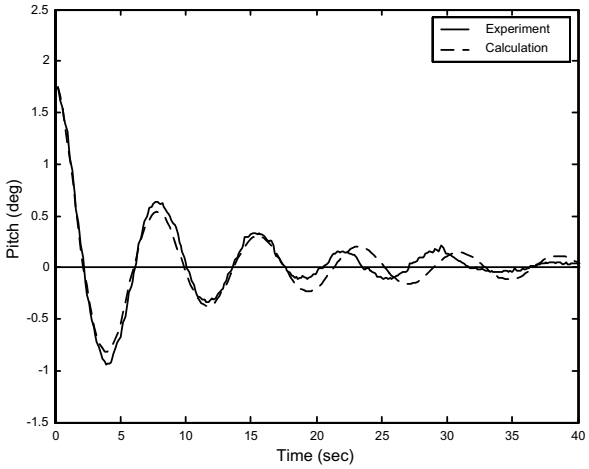

Fig. 7 Pitch free-decay test for freely floating case: solid line = experiment, dashed line = calculation

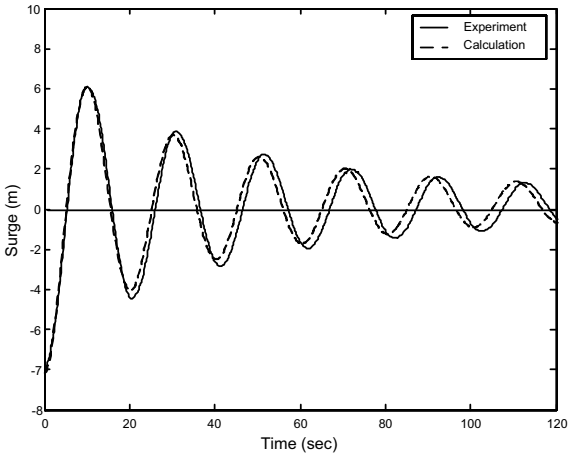

Fig. 8 Surge free-decay test for moored case: solid line = experiment, dashed line = calculation

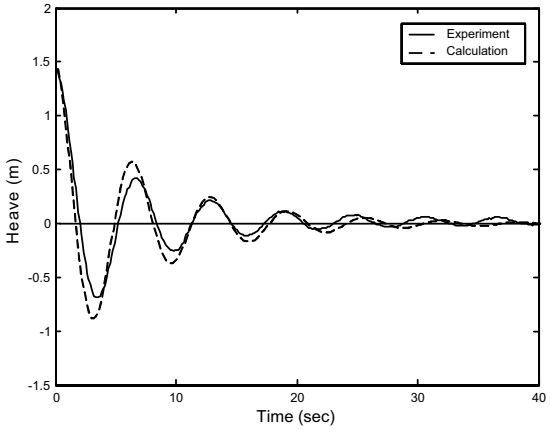

Fig. 9 Heave free-decay test for moored case: solid line = experiment, dashed line = calculation

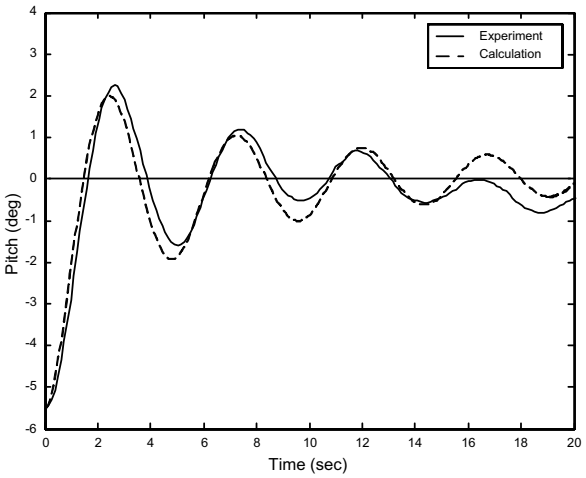

Fig. 10 Pitch free-decay test for moored case: solid line = experiment, dashed line = calculation

Motion RAO were extracted for both regular and irregular wave cases. The waves are incident head-on for all cases. Data obtained from the model tests and shown in the figures are extracted from six 6 seastates with peak periods, Tp = 4.5, 6, 8, 9, 11 and 15 s, respectively.

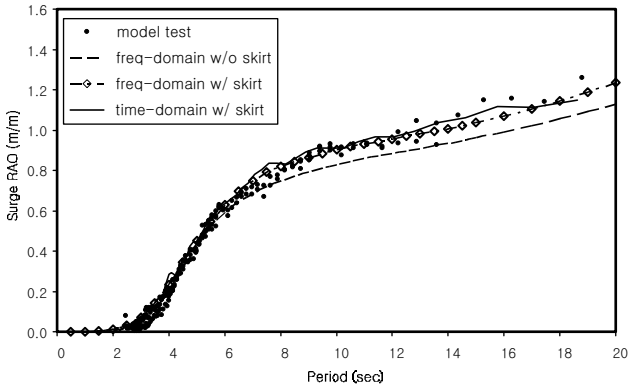

Fig. 11 Surge RAO for freely floating case: dot = model test, dashed line = freq domain w/o skirt, solid line = time domain w/skirt, dash & dot = freq domain w/skirt

Figs. 11∼13 present the comparisons for the surge, heave and pitch RAO for the freely floating buoy (horizontal mooring). Figs. 14∼16 present the same information for the moored buoy (1000 m). The figures are arranged to allow direct comparison of the results from the 2 cases; however, note that the scale is not the same for each case. The figures compare the model test data to numerical simulations carried out in both the time and frequency domain. Two sets of frequency-domain results are provided: from

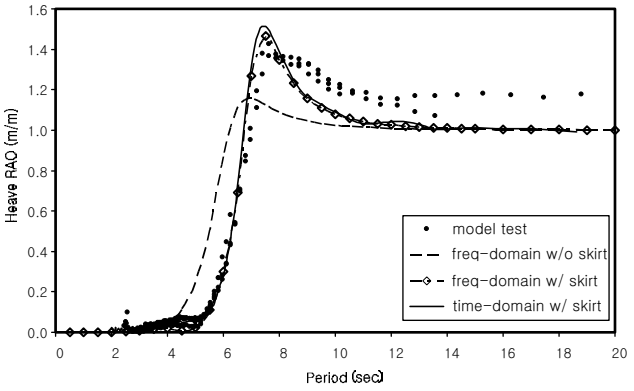

Fig. 12 Heave RAO for freely floating case: dot = model test, dashed line = freq domain w/o skirt, solid line = time domain w/skirt, dash & dot = freq domain w/skirt

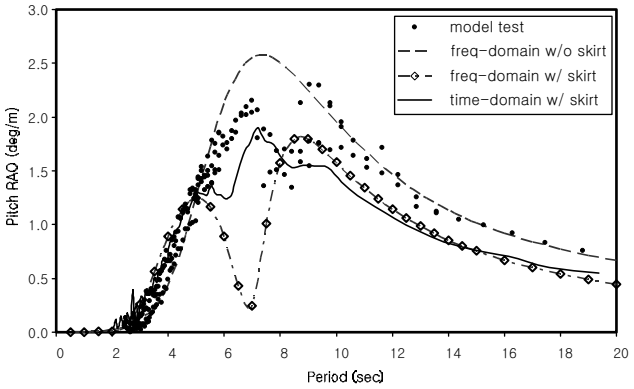

Fig. 13 Pitch RAO for freely floating case: dot = model test, dashed line = freq domain w/o skirt, solid line = time domain w/skirt, dash & dot = freq domain w/skirt

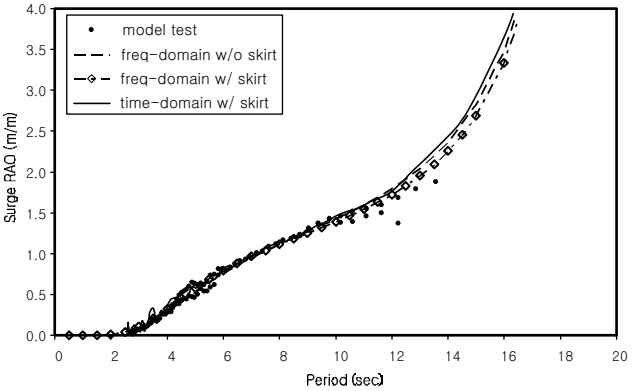

Fig. 14 Surge RAO for moored case: dot = model test, dashed line = freq domain w/o skirt, dash & dot = freq domain w/skirt, solid line = time domain w/skirt

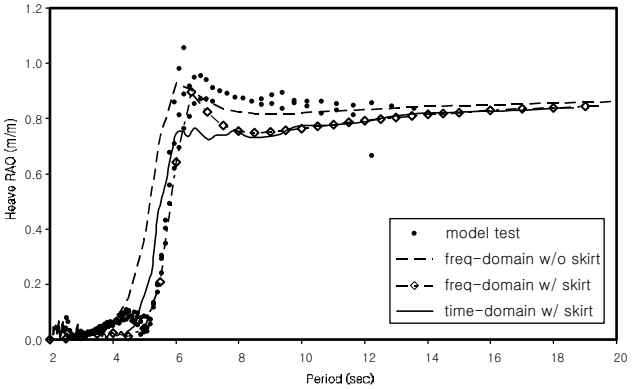

Fig. 15 Heave RAO for moored case: dot = model test, dashed line = freq domain w/o skirt, dash & dot = freq domain w/skirt, solid line = time domain w/skirt

a diffraction analysis conducted without modeling the skirt (freq-domain w/o skirt), and from a diffraction analysis with a correction for the added mass and damping generated by the skirt.

Fig. 11 presents the surge RAO for the freely floating case and shows that all 3 numerical models match the data well. Fig. 14 presents the surge RAO for the moored buoy. Note that the surge natural period is at 19 s, and its influence on the surge response

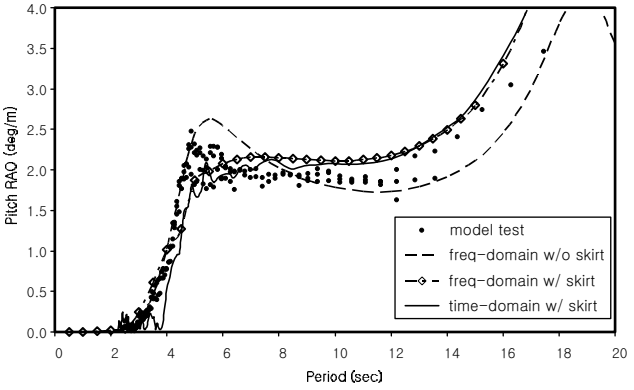

Fig. 16 Pitch RAO for moored case: dot = model test, dashed line = freq domain w/o skirt, dash & dot = freq domain w/skirt, solid line = time domain w/skirt

is observed at the lower periods. Compared to Fig. 11 the moored buoy has a larger surge response than the free-floating buoy.

Figs. 12 and 15 present the heave RAO of the freely floating and moored buoys, respectively. As expected, the numerical model that did not account for the skirt does not match the data well. However, the numerical models with the skirt model implemented provide an adequate representation of the model test response. Note that the moored buoy has a reduced heave response compared to the free-floating buoy, and that the predicted response is a bit lower than that measured. Figs. 13 and 16 present the pitch RAO of the freely floating and moored buoy, respectively.

Note that Fig. 16 illustrates the coupling between surge and pitch for the moored buoy and its influence on the overall pitch response that is greater than that of the free-floating buoy. This demonstrates the importance of the mooring and flowline system on the buoy response, and the influence of the added mass and damping of the lines not considered here (due to the small diam of the model test mooring lines).

CONCLUSIONS AND FUTURE WORK

This paper presents a time-domain coupled analysis of a deepwater oil offloading buoy with emphasis on better buoy pitch motion prediction with viscous modeling of the buoy skirt compared to frequency-domain analysis with a linearized mooring stiffness. The hydrodynamic characteristics of the buoy model and the skirt viscous modeling were addressed. To estimate the overall damping amount of the entire system, free-decay tests for surge, heave and pitch motions were conducted.

Both frequency- and time-domain approaches were presented and compared. To validate the suggested numerical modeling, 2 sets of model tests, a freely floating case and a moored case, were carried out and analyzed. Based on analyzed comparisons, the following conclusions can be reached:

- In the cases where the skirt was not modeled in the hydrodynamic model, the corrections to the heave and pitch added-masses should be evaluated in order to obtain an accurate estimation of the heave and pitch natural periods.
- In the freely floating case where the time-domain analysis with skirt viscous modeling is a better predictor of the pitch motion around the natural period than the frequency-domain analysis based on a linearized stiffness, which produces a deep valley in a pitch motion RAO due to wave exciting pitch moment cancellation, resulting from the existence of a skirt in the diffraction/radiation model.
- Because of the size of a buoy, the inertia effect on buoy hull can be dominant; however, the viscous effect on a skirt influences heave and pitch motion responses in a natural period region.
- Skirt radiation damping is negligible compared to skirt viscous damping.
- Estimating the viscous drag coefficient of the disks surrounding the buoy hull is the key to matching both the heave and pitch motions of the buoy.

In this study the viscous modeling of the buoy hull was based on a quadratic form of the absolute velocity. Topics of future work are quantitative comparison of relative velocity-based and absolute velocity-based viscous modeling and the linearization of nonlinear drag terms for a better frequency-domain analysis. As the skirt viscous damping plays an important role in determining the buoy response, a more detailed study in defining the optimum damping to minimize buoy heave and pitch motions is of interest.

ACKNOWLEDGEMENTS

The authors are very grateful to the management of FMC Technologies Floating Systems Inc. for their support and permission to publish this paper.

REFERENCES

Bunnik, THJ, de Boer, G, Cozijn, JL, van der Cammen, J, van Haaften, E, and ter Brake, E (2002). "Coupled Mooring Analysis in Large Scale Model Tests on a Deepwater CALM Buoy in Mild Wave Conditions," *Proc Offshore Mech & Arct Eng*, Oslo, CD-ROM Paper No OMAE28056.

Colbourne, DB (2000). "Deep Water CALM Buoy Moorings Wave Basin Model Tests," *Tech Rept*, Inst for Marine Dynamics, Nat Res Council Canada, TR-2000-06.

Cozijn, JL, and Bunnik, THJ (2004). "Coupled Mooring Analysis for a Deep Water CALM Buoy," *Proc Offshore Mech & Arct Eng*, CD-ROM Paper No OMAE2004-51370, Vancouver, Canada.

Garret, DL (2005). "Coupled Analysis of Floating Production Systems," *Ocean Eng*, Vol 32, pp 802–816.

Heyl, CN, Zimmermann, CA, Eddy, SL, and Duggal, AS (2001). "Dynamics of Suspended Mid-Water Flowlines," *Proc Offshore Mech & Arct Eng*, CD-ROM Paper No OMAE01-1167, Rio de Janeiro.

Hwang, Y-L (1997). "Dynamic Analysis for the Design of CALM System in Shallow and Deep Waters," *J Offshore Mech and Arct Eng*, Vol 119, pp 151–157.

Korsmeyer, FT, Lee, C-H, Newman, JN, and Sclavounos, PD (1988). "The Analysis of Wave Interactions with Tension Leg Platforms," *Proc 7th Int Conf Offshore Mech & Arct Eng,* JS Chung and SK Chakrabarti, eds, ASME, New York, pp 1–14.

Leonard, JW, Idris, K, and Yim, SCS (2000). "Large Angular Motions of Tethered Surface Buoys," *Ocean Eng*, Vol 27, pp 1345–1371.

Ormberg, H, and Larsen, K (1998). "Coupled Analysis of Floater Motion and Mooring Dynamics for a Turret-Moored Ship," *Appl Ocean Res*, Vol 20, pp 55–67.

Principia RD & IFP (2004). *DeepLines v4r1 Theory Manual*.

Ryu, S, and Kim, MH (2003). "Coupled Dynamic Analysis of Thruster-Assisted Turret-Moored FPSO," *OCEANS 2003*, San Diego, MTS, pp 1613–1620.

Sagrilo, LVS, Siqueira, MQ, Ellwanger, GB, Lima, ECP, Ferreira, MDAS, and Mourelle, MM (2002). "A Coupled Approach for Dynamic Analysis of CALM Systems," *Appl Ocean Res*, Vol 24, pp 47–58.

Valliet, F, Cuenca, A, and Le Buhan, P (2002). "JIP CALM Buoy Model Test Results and DeepLines Calibration," *Tech Rept*, Principia RD Ret.25.084.01.